SOME ASPECTS OF THE A.C. IMPEDANCE BEHAVIOUR OF NICKEL HYDROXIDE AND NICKEL/COBALT HYDROXIDE ELECTRODES IN ALKALINE SOLUTION

R. D. ARMSTRONG and E. A. CHARLES

Electrochemistry Research Laboratories, Bedson Building, University of Newcastle upon Tyne, Newcastle upon Tyne NE1 7RU (U.K.)

(Received November 17, 1988)

Summary

The a.c. impedance spectra have been determined, across the nickel/cobalt hydroxide range, for thin film electrodes. The electrodes were prepared by cathodic deposition and spectra were obtained under various conditions of charge and discharge, by application of sequential d.c. potential steps.

Estimates of the electrode surface area showed that the thin film microporosity is increased by the addition of cobalt, reaching a maximum at cobalt levels greater than 15%. The surface area results have been related to the electrode performance and the extension of the redox potential region, with increasing cobalt content, has been confirmed by the spectra observed.

Introduction

The addition of cobalt to the positive electrode of the nickel—cadmium cell was first commercially exploited by Edison at the beginning of this century [1] and interest in the additive has continued ever since [2].

Many physical techniques have been employed in the study of the nickel/cobalt hydroxide system; but the results have not always been clear due to the complexity of the cells being examined. Researchers have studied complete batteries, single cells and individual electrodes. With the development of a consistent cathodic deposition process, pioneered by Briggs and Wynne-Jones [3], many workers turned to the examination of thin film electrodes. These electrodes have a relatively simple geometry and thus should exhibit some of the more fundamental characteristics of the system.

In this study we have attempted to clarify some of the properties of such thin films and the effects of cobalt upon them. An a.c. impedance technique [4] has been used, which allows *in situ*, quasi steady-state, measurements to be made and when coupled with other techniques the power of this research tool has proved valuable in illuminating the nature of the nickel/cobalt hydroxide film.

0378-7753/89/$3.50

Over the last ten years several papers have been published on the impedance behaviour of thin film electrodes [5 - 7] and also on small sintered plates [8]. The resulting information is incomplete and comparatively few experimental results have been published, some authors relying upon theoretical, analogous, circuits to describe their ideas as to what results might be obtained from the real system. Whilst acknowledging the experimental difficulties and problems in data interpretation when using this technique, experimental backing to any theory of this complex electrode system is necessary. It is hoped that the present work may contribute to solving some of the characteristics of the electrode behaviour.

For an electrode of the $Ni/Ni(OH)_2/KOH_{(aq)}$ type, as illustrated in Fig. 1, the electrode impedance would have contributions from the bulk $Ni(OH)_2$ phase, the bulk $KOH_{(aq)}$ phase and from the two interfaces [$Ni/Ni(OH)_2$ and $Ni(OH)_2/KOH_{(aq)}$]. The bulk phases would lead to a high frequency resistive offset on the real axis of the resulting impedance diagram, corresponding to the total resistance between the tip of the reference electrode luggin and the nickel substrate, as indicated in Fig. 2. If the nickel hydroxide film was porous, and was penetrated by the electrolyte, then little of its resistance would be apparent; in effect, the aqueous KOH would short most of it out. Even if the cathodically-deposited film was highly porous, however, it is unlikely that the electrolyte would contact the substrate directly because of the presence of a layer of nickel hydroxide, a few atomic-layers thick, which is readily formed at the interface.

At low frequencies the impedance spectra would be dominated by interfacial impedances. For the case of slow electron transfer across the $Ni/Ni(OH)_2$ interface, as illustrated in Fig. 1a (or possibly when no electron transfer occurs at this interface) coupled with rapid OH^- equilibration across

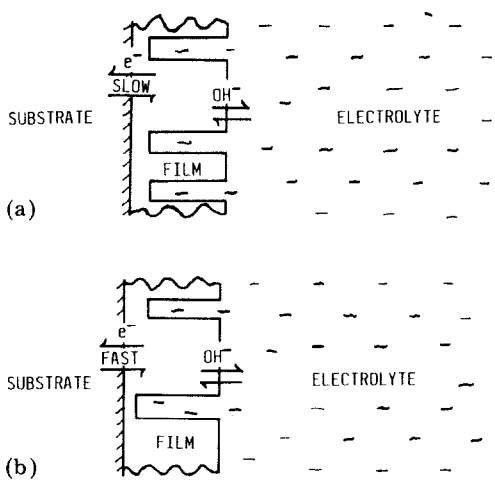

Fig. 1. Schematic diagram of the reactions at a thin film $Ni/Ni(OH)_2$ electrode in KOH electrolyte.

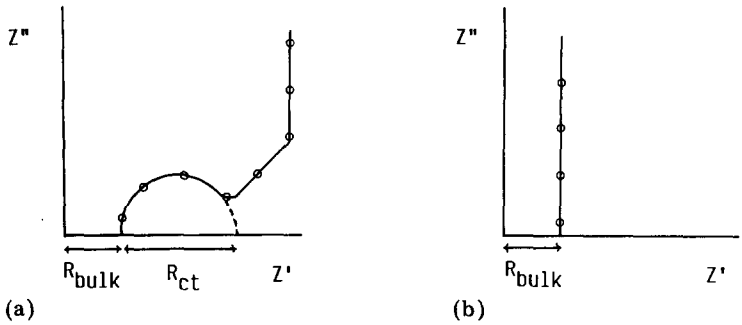

Fig. 2. Idealised impedance spectra showing the effect of changes in R_{ct}.

the $Ni(OH)_2/KOH_{(aq)}$ interface, the low frequency impedance would be due to the $Ni/Ni(OH)_2$ junction. This would in general have the form shown in Fig. 2a, where, after the offset due to the bulk phase resistance, we would expect to find a charge transfer resistance, R_{ct}, for electron transfer at the $Ni/Ni(OH)_2$ interface, in parallel with a capacitive region, C_{dl}, for the $Ni/Ni(OH)_2$ interface. At very low frequencies a Warburg-type impedance (due to diffusion of the redox components in the nickel hydroxide phase) would be likely to be present. This Warburg impedance would terminate in a capacitive line due to finite diffusion effects in the $Ni(OH)_2$ phase. When $R_{ct} \rightarrow \infty$, the impedance spectrum shown in Fig. 2a would collapse to that illustrated in Fig. 2b, giving, at low frequencies, a capacitive line from which the electrode double layer capacitance, C_{dl}, could be estimated.

When rapid electron transfer occurs at the $Ni/Ni(OH)_2$ interface and slow OH^- transfer takes place at the $Ni(OH)_2/KOH_{(aq)}$ interface, as shown in Fig. 1b, impedance diagrams similar to those illustrated in Fig. 2 would again be expected, except that (i) all interfacial quantities would relate to the $Ni(OH)_2/KOH_{(aq)}$ interface and (ii) the rough nature of the interface would introduce further complications. However, when $R_{ct} \rightarrow \infty$, then C_{dl} would, at sufficiently low frequencies, give a measure of the interface area. This is generally done by assuming that a flat surface has a C_{dl} value of approximately 50 uF cm^{-2} [9]. Thus, for example, if a thin film electrode had a capacitance of 100 uF per cm^2 of substrate we may deduce that the film porosity has approximately doubled the solid/solution interface area, providing that the electrode reacts by a mechanism where the hydroxide ion exchange is the rate determining step as illustrated in Fig. 1b.

When making surface area estimates, however, the frequency at which the interfacial capacitance is determined must also be taken into consideration. Basically, at high frequencies, only large geometrical features contribute to the capacitance: that is to say, the interior of any small pores or defects are not seen electrically at these frequencies because ion migration in or out of these features takes a finite time. At lower frequencies, smaller features will begin to contribute to the interfacial capacitance, resulting in

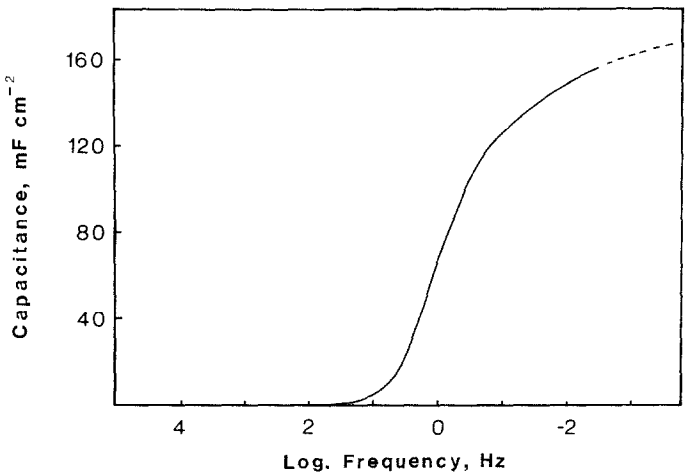

Fig. 3. Typical change in interfacial capacitance, in mF cm^{-2} of substrate, with a.c. impedance measurement frequency. (In this case for 60% Co, beta-phase, thin film at 380 mV.)

more accurate surface area estimates. A more detailed account of the effects of electrode porosity has been reported by De Levie [10].

The typical effect of measurement frequency upon the interfacial capacitance of a porous electrode, with blocked charge-transfer, is illustrated in Fig. 3. At high frequencies the detection system does not see the true porosity of the electrode and records a capacitance value close to that of the substrate alone, whereas at low frequencies an increasingly accurate measure of the electrode porosity is obtained. At infinitely low frequencies the capacitance would become constant and the highest, most accurate, surface area estimates would be made.

The model described above was applied to the data collected, so that geometric surface area estimates for the film could be determined.

Experimental

Electrodes were prepared from 0.5 cm diameter nickel rod, which was heat sealed into polypropylene holders so as to expose an area of approximately 1.8 cm^2. A nickel hydroxide or homogeneous nickel and cobalt hydroxide film was electrodeposited onto this substrate by cathodic polarisation at 1 mA cm^{-2} for 10 min from a 0.05 M nickel nitrate solution or a 0.05 M nickel and cobalt nitrate solution respectively. This produces a thin film deposit (calculated to be 2×10^{-4} cm thick) of hydrated, alpha-phase, material. The weight of alpha-phase nickel hydroxide deposited was calculated to be 0.71 mg and was kept constant so that relative surface area ratios could be established. The electrodes were then given a single constant

current charge and discharge at 0.2 mA cm^{-2}, in 5 M KOH to oxidise any cobalt present to the Co(III) state.

To prepare beta phase material, normally found in commercial batteries, the electrodes were then placed in a PTFE vessel containing 5 M KOH, or 5 M KOH saturated with cobalt, and stored for 120 h at a temperature of 40 °C. After ageing, the electrodes were given a further constant current cycle, ensuring complete discharge of the electrode.

A brief examination of anodically-formed thin films (≈50 Å thick [11]) was made. These were prepared on the same electrode substrates by polarising the nickel to 550 mV (Hg/HgO) for 3 h in 5 M KOH.

The cell used for the a.c. impedance measurements consisted of a single glass chamber of 150 cm^3 volume, into which were sealed a cylindrical, platinum, counter electrode and a glass luggin capillary. The working electrode was placed centrally in the chamber and an external Hg/HgO reference electrode was attached by a capillary to the cell. Analar KOH (5 M) was used both in the cell and in the reference electrode for all of the measurements.

Starting from a discharged condition, impedance measurements were made, with a frequency response analyser, at a series of potentials up to the point at which oxygen evolution began. A further set of data was then recorded at similar points during discharge. At each potential selected, the electrode was allowed to approach equilibrium for at least 15 min, prior to any data being collected (the length of time depending upon the approach of the current flow to zero). The system was controlled by a microcomputer which was also used to analyse the results. Spectra were obtained over the range 100 kHz to 5 mHz at regular intervals of applied d.c. potential.

Results

Figure 4 shows a series of typical impedance spectra for 0% and 12% Co, beta-phase, thin film electrodes. This data was taken during a series of discharge potential steps, but was essentially the same as the charging step spectra, when the potential hysteresis of the electrode is taken into account. At an applied d.c. potential of 500 mV both electrodes were fully charged and oxygen evolution was commencing on the thin films. This charge-transfer reaction [12] would be expected to give rise to a semicircle in the impedance plane; however, in Fig. 4, only the first part of the semicircle is observed due to its large diameter. Below the oxygen evolution potential a capacitive impedance spectrum was seen for both electrodes, the potential being too high to allow any reduction of the active material to occur at the electrode. As the potential was lowered the reduction process could begin, and at around 320 mV spectra showing a charge-transfer semicircle and a Warburg-type line were recorded. The presence of a Warburg line indicated that the reaction process was partially diffusion controlled. At lower potentials the electrodes became capacitive again, corresponding to the discharged condition; however, because cobalt addition both lowers the

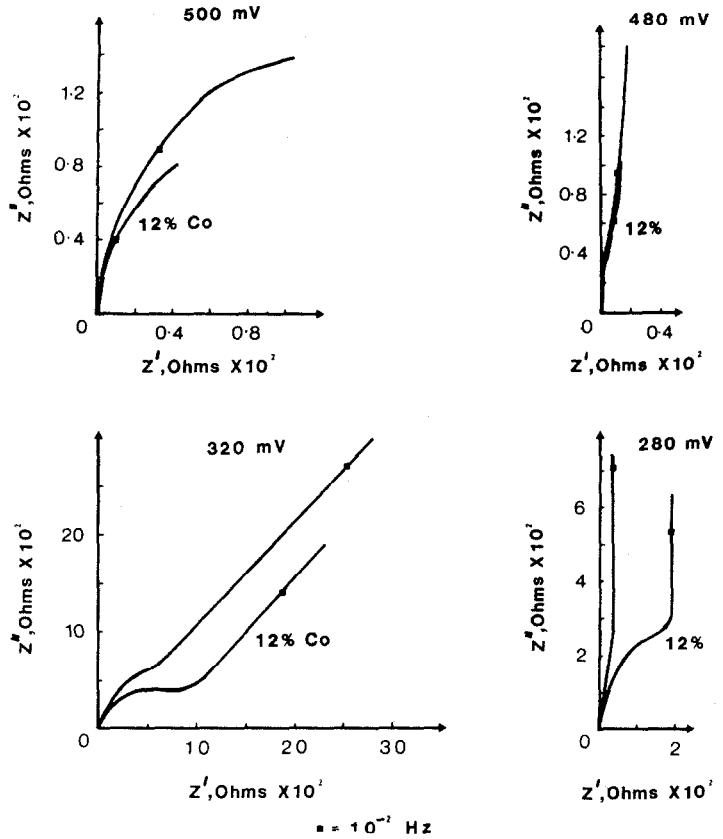

Fig. 4. Typical impedance spectra for 0% and 12% cobalt thin film electrodes at 500 mV, oxygen evolution; 480 mV, charged; 300 mV Redox reaction; and 280 mV, discharged.

redox potential and extends the range over which the redox reaction can occur [13], Fig. 4 shows that some reaction is still indicated for the 12% cobalt film at 280 mV. The 12% cobalt electrode behaves completely capacitively when the applied potential is approximately 150 mV.

It may be noted that in all cases the bulk resistance (due to the solution and film) was less than 0.5 ohms, which indicates that the electrolyte always penetrated the film to a considerable extent.

The Figure shows that at low levels of cobalt there is no great change in the impedance behaviour of the electrodes.

Table 1 lists high frequency interfacial capacitance data for thin film, cathodically deposited, electrodes. It can be seen that all the electrodes exhibit a higher capacitance when near the fully charged condition than when discharged. It is known that the nickel component of the film has a considerably lower conductivity when in the reduced, Ni(II), state than when oxidised [13] and thus the discharged electrode may well exhibit a

TABLE 1

High frequency capacitance values for thin film electrodes determined from impedance measurements at 5000 Hz

Potential (mV) *vs.* (Hg/HgO)	Interfacial capacitance (mF cm^{-2})			
	Alpha $Ni(OH)_2$ film	Beta $Ni(OH)_2$ film	12% Cobalt, beta film	60% Cobalt, beta film
Charging				
330	0.24	0.29	0.24	0.12
380	0.32	0.88	0.49	0.16
430	1.0	0.26	0.83	0.25
480	5.0	1.9	1.8	0.31
500		2.9	1.8	0.38
Discharging				
480		3.4	5.1	0.36
430	5.7	0.35	4.8	0.38
380	4.0	0.32	2.9	0.31
330	3.0	0.22	0.87	0.26
300	0.65	0.73	0.23	0.29
280	0.22	0.15	0.20	0.21

capacitance mainly due to the substrate surface. Similarly, the oxidised film might yield a capacitance for the entire film/electrolyte interface, the increased conductivity of the active mass possibly allowing the electron exchange at the substrate to become faster. The addition of cobalt to the system enhances the electrode film conductivity and would thus decrease the variation of capacitance with state of charge, as can be seen in Table 1, particularly for the 60% cobalt electrode. This behaviour is illustrated in Fig. 5, where the electrode capacitance is plotted against measurement frequency for electrode potentials above and below the Ni(II)/Ni(III) redox potential. The marked decrease in capacitance upon reduction of the nickel hydroxide electrode contrasts strongly with the cobalt-containing electrode, where a small hysteresis, is observed.

Table 2 shows the corresponding low frequency capacitance data at various stages of charge and discharge. The electrode capacitance values are approximately one thousand times larger than at the high frequency, which indicates considerable microporosity, as outlined earlier. A maximum in interfacial capacitance was, again, observed when the electrodes were in an oxidised condition and addition of cobalt clearly decreases the capacitance variation with state of charge.

For nickel hydroxide and low cobalt containing nickel hydroxide electrodes, the impedance measurements around the redox potential could not be used to give capacitance data for Table 2 because the capacitive component of the spectra is beyond the Warburg-type line, at a very low

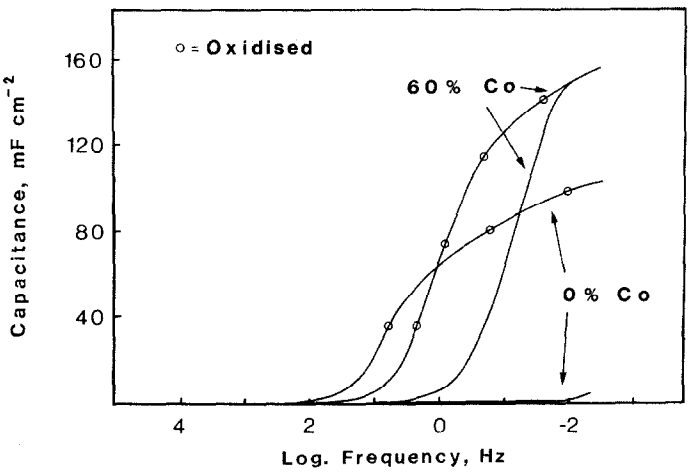

Fig. 5. Typical variation of interfacial capacitance, in mF cm^{-2} of substrate, with a.c. impedance measurement frequency for 0% and 60% cobalt electrodes at potentials above and below the Ni(II)/Ni(III) redox potential.

TABLE 2

Low frequency capacitance values for thin film electrodes determined from impedance measurements at 0.01 Hz

Potential (mV) *vs.* (Hg/HgO)	Interfacial capacitance (F cm^{-2})			
	Alpha $Ni(OH)_2$ film	Beta $Ni(OH)_2$ film	12% Cobalt, beta film	60% Cobalt, beta film
Charging				
330		Redox semi-circle and Warburg		0.17
380				0.17
430	0.059	0.0075	0.28	0.20
480	0.098	0.12	0.24	0.16
500		Oxygen evolution		0.14
Discharging				
480	0.098	0.096	0.22	0.15
430	0.11	0.099	0.24	0.16
380	0.12	0.016	0.28	0.17
330	0.096			0.10
300		Redox semi-circle and Warburg		0.11
280	0.0013	0.0013	0.0011	0.14

frequency, and would reflect the charge/discharge process as well as the surface area.

As mentioned earlier, cobalt increases the potential range over which the redox process can occur and this has been reflected in the impedance

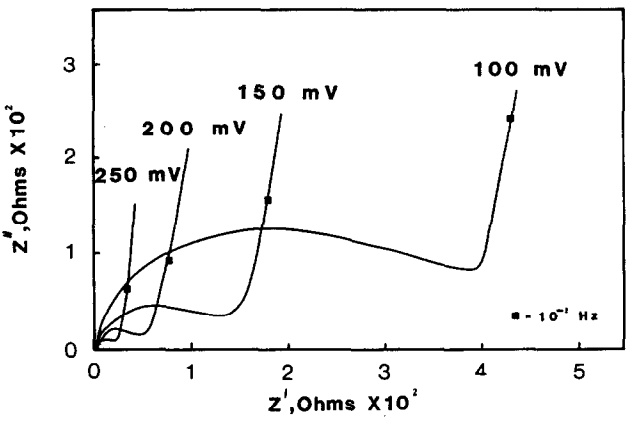

Fig. 6. Impedance spectra for a 60% Co, beta-phase, thin film electrode, showing the effect of d.c. potential upon the redox process.

spectra observed. Figure 6 shows typical spectra for a 60% cobalt, beta phase, film under various d.c. potentials.

It is apparent that at these high cobalt levels there is no visible Warburg-type line associated with the redox process and this suggests that the reaction is no longer dominated by diffusion effects, the decrease in diffusion control perhaps being a result of the changes in film morphology or conductivity resulting from cobalt addition. It should be noted that a Warburg line can, on occasion, be obscured by a large charge-transfer semicircle, although this is considered unlikely here.

It can be seen that a trend in the magnitude of the charge-transfer resistance, R_{ct}, with potential exists, such that at potentials on the edge of the redox potential region, R_{ct} is large, but when the electrode is near the nickel redox potential, R_{ct} becomes very small. This effect was also observed at low cobalt levels, R_{ct} changing by up to a factor of one hundred over the potential range where redox occurred. This change in R_{ct} is in agreement with Barton *et al.* [8] who computed results for a sintered electrode.

Essentially, when R_{ct} becomes very large, a capacitive impedance spectrum is observed, being the stem of the semicircle, which is so large as to be beyond the detection range of the equipment. Now, for a 60% Co electrode, because the redox potential range is extended, a series of charge-transfer semicircle spectra can be obtained, the R_{ct} values becoming smaller as the potential of the nickel redox maximum is approached and larger further away from the redox potential. Thus, if the electrode was taken to more cathodic potentials than applied in Fig. 4, then a capacitive spectrum would eventually be recorded, just as in the case of the low cobalt electrodes. It may also be noted that at high cobalt levels the R_{ct} values are generally smaller than at low cobalt levels, allowing for redox potential shift, which indicates that cobalt improves the reaction kinetics of the electrode.

This observation is in agreement with the findings of several workers, including Elder and Jost [14].

Discussion

The electrode capacitance results obtained may be interpreted in the following way. Considering a pure nickel hydroxide electrode in the reduced state, the measurements indicate that it has a low interfacial capacitance over a considerable frequency range, which is not much larger than a typical double layer capacitance. This behaviour is consistent with a mechanism where the low conductivity of the film may result in electron exchange at the film/substrate interface becoming the rate determining step (see Fig. 1a). The capacitance values obtained under these conditions would be thus related to the geometric area of the substrate alone. The impedance measurements obtained do, however, show some suggestion of film porosity, in that there is no significant bulk resistance observed.

When the electrode is oxidised to some extent, or when cobalt is added to the lattice, an increase in film conductivity occurs which may result in the hydroxide ion exchange becoming rate determining, as described earlier. The impedance behaviour observed would then be dependent upon the electrolyte/film interface and would result in much larger capacitance values which may be related to the surface area of the interface.

Table 3 shows the derived surface area ratios along with some electrode capacity data for comparison. The anodic film data cannot be compared directly with the cathodically-deposited electrode results, because the quantity of material present is somewhat less: however, it is apparent that the anodic films are micro-porous to an extent which may not be fully

TABLE 3

Relative surface area ratios from impedance data and electrode capacity results

Electrode type	Ni rod	Anodic film 0% Co	Cathodically deposited films, β-phase				
			0% Co	12% Co	45% Co	60% Co	100% Co
Film surface area[a], cm^2 per cm^2 of substrate							
At 0.01 Hz	1	400	632	1474	1263	1053	947
At 5000 Hz	1	28	17	25	60	2	2
Electrode capacity, mC per cm^2 of substrate							
Constant *I* charging	0		238	337	407	280	0
Linear *E* Sweep	0		194	245	390	210	0

[a]Values corrected by Ni rod capacitance value.

appreciated from scanning electron microscope (SEM) examination [15]. The cathodically-formed films show some correlation between electrode capacity and relative surface area. The exact relationship is unclear because cobalt is essentially an electrocatalyst in this system: when substituted for the nickel component, beyond the level at which maximum utilisation of the active material occurs, it will effectively decrease the electrode capacity regardless of the surface area exposed [13].

The electrode capacity is thus dependent upon the amount of active material present and the extent to which it is utilised, whether the change in utilisation is due to improved conductivity or to an enlarged film/electrolyte interface.

The surface area ratios are complementary to our previous SEM studies of these electrodes which showed considerable morphological changes with cobalt addition [16]. It may be noted that the surface area ratios for the cathodically deposited films results in surface area per gramme values around 150 $m^2\ g^{-1}$ which may be compared with approximately 210 $m^2\ g^{-1}$ for sintered plate electrodes [17].

The impedance data presented has allowed the qualitative, SEM, studies of cathodically-deposited thin film electrodes, made earlier, to be quantified in terms of changes in surface area. The highly porous nature of the electrodes has been demonstrated and the surface area ratios agree well with BET measurements reported elsewhere [15].

The trends in electrode capacitance with oxidation state are in agreement with the literature [5, 6] and are consistent with our earlier observation of enhanced film conductivity due to the presence of cobalt.

The addition of cobalt to the system considerably extends the potential range over which redox behaviour may occur and this is essentially complementary to our earlier linear potential sweep experiments [16] as shown in Fig. 7. The linear sweep results did, however, exhibit one feature which has not been mirrored in the present work and this is concerned with a two-step oxidation process observed around the 50% cobalt level. Figure 7 shows typical linear sweep curves for a 45% and a 75% cobalt electrode: as can be seen there is clear evidence here for a two stage redox process at the 45% level and it may have been expected that impedance studies would also show such details. A series of spectra were envisaged comprising two regions where charge-transfer semicircles would be seen, separated by a region with a capacitive spectrum. However, no such results were obtained, there being a continuous series of redox, semicircle, spectra across the relevant potential region. This indicates that the two oxidation and reduction steps are not truly independent of each other, that is to say, the Ni(II)/Ni(III) redox potential region overlaps with the Ni(III)/Ni(IV) redox region.

Finally, the current work has shown that the impedance technique can be applied to determine surface area estimates and to provide information upon the reaction kinetics. It is apparent from the study that even thin film electrodes, used for battery research because of their relative simplicity, are actually quite complex in their own right and deserve closer study. Indeed

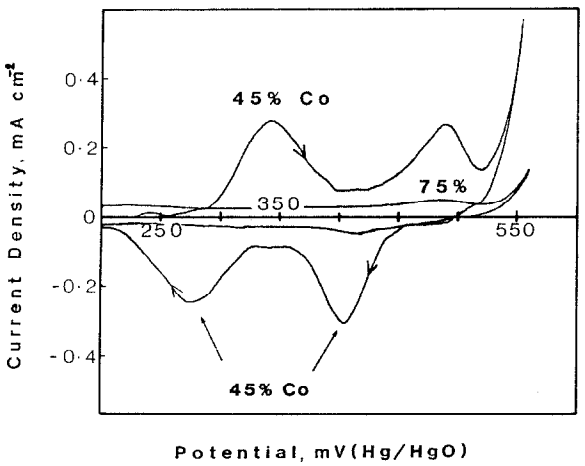

Fig. 7. Linear potential sweep curves for beta-phase thin film electrodes containing 45% and 75% cobalt, after several cycles at 0.1 mV s^{-1}.

these highly porous electrodes have physical characteristics similar to those of the complex sintered nickel electrodes used in the battery industry today [18].

Conclusions

1. Thin film electrodes prepared anodically and cathodically have been shown to be micro-porous. In the case of cathodically formed films, this porosity is related to cobalt content and may be advantageous in commercial electrodes.

2. A relationship between electrode surface area and electrode capacity exists, which is complicated by the presence of cobalt due to increased film conductivity and by changes in the amount of active material deposited.

3. The addition of cobalt to the system improves the electrode kinetics by lowering the charge-transfer resistance of the reaction process.

Acknowledgements

The authors would like to thank Alcad Ltd. for funding the project, along with Mr J. Parker and Dr G. W. D. Briggs who gave much assistance during the course of this research.

References

1 T. A. Edison, *U.S. Patent 1,083,356* (June 1914).
2 S. Uno Falk and A. J. Salkind, *Alkaline Storage Batteries*, Wiley, New York, 1969.

3 G. W. D. Briggs and W. F. K. Wynne-Jones, *Electrochim. Acta, 7* (1962) 241.
4 M. Sluyters Rehbach and J. H. Sluyters, *Electroanalytical Chemistry*, Vol. 4, Marcel Dekker, New York, 1970, Ch. 1.
5 S. H. Glarum and J. H. Marshall, *J. Electrochem. Soc., 129* (1982) 535.
6 M. J. Madou and M. C. H. McKubre, *J. Electrochem. Soc., 130* (1983) 1056.
7 A. H. Zimmerman and P. K. Effa, *J. Electrochem. Soc., 131* (1984) 709.
8 R. T. Barton, M. Hughes, S. A. G. R. Karunathilaka and N. A. Hampson, *J. Appl. Electrochem., 15* (1985) 399.
9 B. E. Conway, *Electrodes Processes*, Ronald Press, New York, 1965.
10 R. de Levie, in P. Delahay (ed.), *Advances in Electrochemistry and Electrochemical Engineering*, Vol. 6, Wiley, New York, 1967, p. 329.
11 J. F. Wolf, L. S. R. Yeh and A. Damjanovic, *Electrochim. Acta, 26* (1981) 409.
12 G. Bronoel and J. Reby, *Electrochim. Acta, 25* (1980) 973.
13 R. D. Armstrong, G. W. D. Briggs and E. A. Charles, *J. Appl. Electrochem., 18* (1988) 215.
14 J. P. Elder and E. M. Jost, *J. Electrochem. Soc., 116* (1969) 687.
15 T. C. Liu and B. E. Conway, *J. Appl. Electrochem., 17* (1987) 983.
16 R. D. Armstrong and E. A. Charles, *J. Power Sources, 25* (1989) 89.
17 P. C. Milner and U. B. Thomas, The nickel—cadmium cell, in C. W. Tobias (ed.), *Advances in Electrochemistry and Electrochemical Engineering*, Vol. 5, Wiley, New York, 1967, p. 1.
18 E. Yeager and A. J. Salkind, *Techniques of Electrochemistry*, Vol. III, Wiley, New York, 1978, Ch. 5, p. 291.